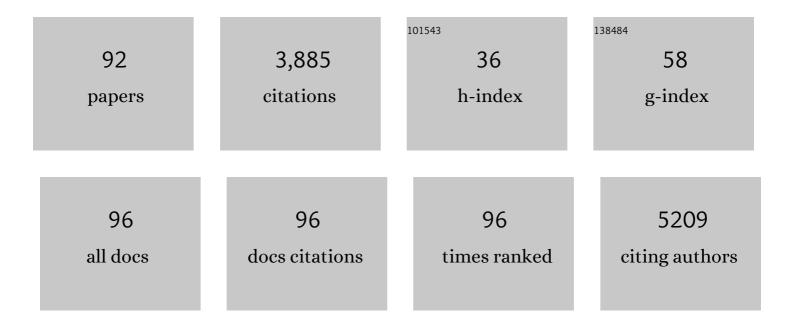
Hengjiang Cong

List of Publications by Year in descending order

Source: https://exaly.com/author-pdf/6809590/publications.pdf

Version: 2024-02-01



#	Article	IF	CITATIONS
1	Electrochemical Oxidative [4+2] Annulation of Different Styrenes toward the Synthesis of 1,2-Dihydronaphthalenes. CCS Chemistry, 2022, 4, 1557-1564.	7.8	15
2	Electrochemical dual-oxidation strategy enables access to α-chlorosulfoxides from sulfides. Science Bulletin, 2022, 67, 79-84.	9.0	24
3	Nitridation-induced metal–organic framework nanosheet for enhanced water oxidation electrocatalysis. Journal of Energy Chemistry, 2022, 64, 531-537.	12.9	23
4	Sequence control of metals in MOF by coordination number precoding for electrocatalytic oxygen evolution. Chem Catalysis, 2022, 2, 84-101.	6.1	20
5	Intermolecular Energy Gapâ€Induced Formation of Highâ€Valent Cobalt Species in CoOOH Surface Layer on Cobalt Sulfides for Efficient Water Oxidation. Angewandte Chemie, 2022, 134, .	2.0	39
6	Synthesis of Enantioenriched Fluorinated Enol Silanes Enabled by Asymmetric Reductive Coupling of Fluoroalkylacylsilanes and 1,3-Enynes and Brook Rearrangement. ACS Catalysis, 2022, 12, 2150-2157.	11.2	15
7	Multivariate MOF for optimizing atmospheric water harvesting. Green Energy and Environment, 2022, 7, 575-577.	8.7	7
8	Boosting Hydrogen Oxidation Performance of Phase-Engineered Ni Electrocatalyst under Alkaline Media. ACS Sustainable Chemistry and Engineering, 2022, 10, 3682-3689.	6.7	16
9	Exfoliation of MoS ₂ Nanosheets Enabled by a Redox-Potential-Matched Chemical Lithiation Reaction. Nano Letters, 2022, 22, 2956-2963.	9.1	35
10	Enantioselective Nickel-Catalyzed Reductive Aryl/Alkenyl–Cyano Cyclization Coupling to All-Carbon Quaternary Stereocenters. Journal of the American Chemical Society, 2022, 144, 4776-4782.	13.7	23
11	Selective radical cascade (4+2) annulation with olefins towards the synthesis of chroman derivatives <i>via</i> organo-photoredox catalysis. Chemical Science, 2022, 13, 6316-6321.	7.4	4
12	Electrochemical Oxidative Carbonâ€Atom Difunctionalization: Towards Multisubstituted Imino Sulfide Ethers. Angewandte Chemie - International Edition, 2021, 60, 1573-1577.	13.8	19
13	Electrochemical Oxidative Carbonâ€Atom Difunctionalization: Towards Multisubstituted Imino Sulfide Ethers. Angewandte Chemie, 2021, 133, 1597-1601.	2.0	2
14	Hexagonal RuSe ₂ Nanosheets for Highly Efficient Hydrogen Evolution Electrocatalysis. Angewandte Chemie - International Edition, 2021, 60, 7013-7017.	13.8	88
15	Stereoselective synthesis of 3,3′-pyrrolidinyl-spirooxindoles via the Zn(OAc)2-mediated asymmetric Mannich-type reaction. Tetrahedron Letters, 2021, 67, 152819.	1.4	2
16	β-Substituted Alkenyl Heteroarenes as Dipolarophiles in the Cu(I)-Catalyzed Asymmetric 1,3-Dipolar Cycloaddition of Azomethine Ylides Empowered by a Dual Activation Strategy: Stereoselectivity and Mechanistic Insight. Journal of the American Chemical Society, 2021, 143, 3519-3535.	13.7	34
17	Palladium-Catalyzed (4 + 4) Annulation of Silacyclobutanes and 2-lodobiarenes to Eight-Membered Silacycles via C–H and C–Si Bond Activation. ACS Catalysis, 2021, 11, 5703-5708.	11.2	36
18	Catalytic Synthesis of Atropisomeric <i>o</i> -Terphenyls with 1,2-Diaxes via Axial-to-Axial Diastereoinduction. Journal of the American Chemical Society, 2021, 143, 7253-7260.	13.7	49

#	Article	IF	CITATIONS
19	Manganese-catalyzed chlorosulfonylation of terminal alkene and alkyne via convergent paired electrolysis. Cell Reports Physical Science, 2021, 2, 100476.	5.6	25
20	Copper (II) synergistic AS1411 conjunction with chemical decaging reactions for selective fluorescence imaging and prodrug activation in living systems. Sensors and Actuators B: Chemical, 2021, 349, 130773.	7.8	0
21	Electrochemically selective double C(sp ²)–X (X = S/Se, N) bond formation of isocyanides. Chemical Science, 2021, 12, 14121-14125.	7.4	12
22	Comparative Investigation into Formycin A and Pyrazofurin A Biosynthesis Reveals Branch Pathways for the Construction of <i>C</i> -Nucleoside Scaffolds. Applied and Environmental Microbiology, 2020, 86, .	3.1	15
23	Electrooxidation enables highly regioselective dearomative annulation of indole and benzofuran derivatives. Nature Communications, 2020, 11, 3.	12.8	81
24	One-step rapid synthesis, crystal structure and 3.3 microseconds long excited-state lifetime of Pd1Ag28 nanocluster. Nano Research, 2020, 13, 366-372.	10.4	30
25	Uniform Bi–Sb Alloy Nanoparticles Synthesized from MOFs by Laser Metallurgy for Sodium-Ion Batteries. ACS Sustainable Chemistry and Engineering, 2020, 8, 335-342.	6.7	43
26	Mitigation of voltage decay in Li-rich layered oxides as cathode materials for lithium-ion batteries. Nano Research, 2020, 13, 151-159.	10.4	15
27	Enantioselective Access to \hat{I}^3 -All-Carbon Quaternary Center-Containing Cyclohexanones by Palladium-Catalyzed Desymmetrization. ACS Catalysis, 2020, 10, 216-224.	11.2	21
28	Pd-catalyzed arylation/aza-Michael addition cascade to C2-spiroindolines and azabicyclo[3.2.2]nonanones. Chemical Communications, 2020, 56, 12013-12016.	4.1	8
29	Thermosensitive crystallization–boosted liquid thermocells for low-grade heat harvesting. Science, 2020, 370, 342-346.	12.6	289
30	Twist and sliding dynamics between interpenetrated frames in Ti-MOF revealing high proton conductivity. Chemical Science, 2020, 11, 3978-3985.	7.4	38
31	Synthesis of chiral α-substituted α-amino acid and amine derivatives through Ni-catalyzed asymmetric hydrogenation. Chemical Communications, 2020, 56, 4934-4937.	4.1	19
32	Enantioselective Assembly of Cycloenones with a Nitrile-Containing All-Carbon Quaternary Center from Malononitriles Enabled by Ni Catalysis. Journal of the American Chemical Society, 2020, 142, 7328-7333.	13.7	49
33	Enhancing resistance to radiation hardening and radiation thermal conductivity degradation by tungsten/graphene interface engineering. Journal of Nuclear Materials, 2020, 539, 152348.	2.7	9
34	Stereoselective Palladium-Catalyzed 1,3-Arylboration of Unconjugated Dienes for Expedient Synthesis of 1,3-Disubstituted Cyclohexanes. ACS Catalysis, 2019, 9, 8555-8560.	11.2	39
35	Syntheses and photoluminescence of copper(<scp>i</scp>) halide complexes containing dimethylthiophene bidentate phosphine ligands. New Journal of Chemistry, 2019, 43, 13408-13417.	2.8	24
36	Electrochemical oxidative C–H/S–H cross-coupling between enamines and thiophenols with H ₂ evolution. Chemical Science, 2019, 10, 2791-2795.	7.4	73

#	Article	IF	CITATIONS
37	A new strategy to synthesize three-coordinate mononuclear copper(<scp>i</scp>) halide complexes containing a bulky terphenyl bidentate phosphine ligand and their luminescent properties. New Journal of Chemistry, 2019, 43, 3390-3399.	2.8	23
38	Oxidation-Induced β-Selective C–H Bond Functionalization: Thiolation and Selenation of N-Heterocycles. ACS Catalysis, 2019, 9, 1888-1894.	11.2	41
39	A palladium/norbornene cooperative catalysis to access N-containing bridged scaffolds. Chemical Communications, 2019, 55, 8816-8819.	4.1	24
40	Intramolecular electronic coupling for persistent room-temperature luminescence for smartphone based time-gated fingerprint detection. Materials Horizons, 2019, 6, 1215-1221.	12.2	45
41	Iron-Catalyzed Intramolecular Amination of Aliphatic C–H Bonds of Sulfamate Esters with High Reactivity and Chemoselectivity. Organic Letters, 2019, 21, 2673-2678.	4.6	35
42	Electrooxidative para-selective C–H/N–H cross-coupling with hydrogen evolution to synthesize triarylamine derivatives. Nature Communications, 2019, 10, 639.	12.8	123
43	An Amorphous Cobalt Borate Nanosheet-Coated Cobalt Boride Hybrid for Highly Efficient Alkaline Water Oxidation Reaction. ACS Sustainable Chemistry and Engineering, 2019, 7, 5620-5625.	6.7	51
44	Isolated π-Interaction Sites in Mesoporous MOF Backbone for Repetitive and Reversible Dynamics in Water. ACS Applied Materials & Interfaces, 2019, 11, 973-981.	8.0	25
45	Mesoporous Cages in Chemically Robust MOFs Created by a Large Number of Vertices with Reduced Connectivity. Journal of the American Chemical Society, 2019, 141, 488-496.	13.7	126
46	Electrochemical Oxidative Câ^'H Amination of Phenols: Access to Triarylamine Derivatives. Angewandte Chemie, 2018, 130, 4827-4831.	2.0	42
47	Electrochemical Oxidative Câ^'H Amination of Phenols: Access to Triarylamine Derivatives. Angewandte Chemie - International Edition, 2018, 57, 4737-4741.	13.8	148
48	Mechanically Strong Multifilament Fibers Spun from Cellulose Solution via Inducing Formation of Nanofibers. ACS Sustainable Chemistry and Engineering, 2018, 6, 5314-5321.	6.7	56
49	Metal-organic frameworks for precise inclusion of single-stranded DNA and transfection in immune cells. Nature Communications, 2018, 9, 1293.	12.8	187
50	Enantioselective Construction of Bridgehead Quaternary Carbon Containing Bicyclo[3.3.1]nonanes by Palladium-Catalyzed ÂDesymmetric Arylation. Synthesis, 2018, 50, 1661-1666.	2.3	11
51	π-Extended Benzoporphyrin-Based Metal–Organic Framework for Inhibition of Tumor Metastasis. ACS Nano, 2018, 12, 4630-4640.	14.6	136
52	Redox active ligand and metal cooperation for C(sp ²)–H oxidation: extension of the galactose oxidase mechanism in water-mediated amide formation. Dalton Transactions, 2018, 47, 15293-15297.	3.3	6
53	Iridium-Catalyzed Asymmetric Hydrogenation of Tetrasubstituted α-Fluoro-β-enamino Esters: Efficient Access to Chiral α-Fluoro-β-amino Esters with Two Adjacent Tertiary Stereocenters. Organic Letters, 2018, 20, 6349-6353.	4.6	24
54	Z-Selective Addition of Diaryl Phosphine Oxides to Alkynes via Photoredox Catalysis. ACS Catalysis, 2018, 8, 10599-10605.	11.2	74

#	Article	lF	CITATIONS
55	Ag(I)-Catalyzed Kinetic Resolution of Cyclopentene-1,3-diones. Organic Letters, 2018, 20, 3482-3486.	4.6	16
56	Improved mechanical properties of poly (vinyl alcohol) films with glycerol plasticizer by uniaxial drawing. Polymers for Advanced Technologies, 2018, 29, 2612-2618.	3.2	15
57	Dynamic Hosts for High-Performance Li–S Batteries Studied by Cryogenic Transmission Electron Microscopy and in Situ X-ray Diffraction. ACS Energy Letters, 2018, 3, 1325-1330.	17.4	47
58	Controlling disorder in host lattice by hetero-valence ion doping to manipulate luminescence in spinel solid solution phosphors. Science China Chemistry, 2018, 61, 1624-1629.	8.2	23
59	New Ru(<scp>ii</scp>) N′NN′-type pincer complexes: synthesis, characterization and the catalytic hydrogenation of CO ₂ or bicarbonates to formate salts. New Journal of Chemistry, 2017, 41, 3055-3060.	2.8	25
60	Principles of Designing Extra-Large Pore Openings and Cages in Zeolitic Imidazolate Frameworks. Journal of the American Chemical Society, 2017, 139, 6448-6455.	13.7	197
61	Oxidant-free synthesis of benzimidazoles from alcohols and aromatic diamines catalysed by new Ru(<scp>ii</scp>)-PNS(O) pincer complexes. Dalton Transactions, 2017, 46, 15012-15022.	3.3	28
62	Oxygen Vacancies and Stacking Faults Introduced by Low-Temperature Reduction Improve the Electrochemical Properties of Li ₂ MnO ₃ Nanobelts as Lithium-Ion Battery Cathodes. ACS Applied Materials & Interfaces, 2017, 9, 38545-38555.	8.0	50
63	Spinel-layered integrate structured nanorods with both high capacity and superior high-rate capability as cathode material for lithium-ion batteries. Nano Research, 2017, 10, 556-569.	10.4	26
64	Silver(I)-Catalyzed Atroposelective Desymmetrization of <i>N</i> -Arylmaleimide via 1,3-Dipolar Cycloaddition of Azomethine Ylides: Access to Octahydropyrrolo[3,4- <i>c</i>]pyrrole Derivatives. Journal of Organic Chemistry, 2016, 81, 3752-3760.	3.2	59
65	Deciphering the Spatial Arrangement of Metals and Correlation to Reactivity in Multivariate Metal–Organic Frameworks. Journal of the American Chemical Society, 2016, 138, 13822-13825.	13.7	187
66	Highly Active Carbon Supported Pd–Ag Nanofacets Catalysts for Hydrogen Production from HCOOH. ACS Applied Materials & Interfaces, 2016, 8, 20839-20848.	8.0	53
67	Achieving a balance between small singlet–triplet energy splitting and high fluorescence radiative rate in a quinoxaline-based orange-red thermally activated delayed fluorescence emitter. Chemical Communications, 2016, 52, 11012-11015.	4.1	105
68	Membrane association of SadC enhances its diguanylate cyclase activity to control exopolysaccharides synthesis and biofilm formation in <i>Pseudomonas aeruginosa</i> . Environmental Microbiology, 2016, 18, 3440-3452.	3.8	47
69	Discovery of a ¹⁹ F MRI sensitive salinomycin derivative with high cytotoxicity towards cancer cells. Chemical Communications, 2016, 52, 5136-5139.	4.1	39
70	Structural and Biochemical Insight into the Mechanism of Rv2837c from Mycobacterium tuberculosis as a c-di-NMP Phosphodiesterase. Journal of Biological Chemistry, 2016, 291, 3668-3681.	3.4	67
71	Crystal structure and bonding analysis of the first dinuclear calcium(II)–proton-pump inhibitor (PPI) `butterfly molecule': a combined microcrystal synchrotron and DFT study. Acta Crystallographica Section C, Structural Chemistry, 2016, 72, 326-336.	0.5	Ο
72	Thermal and electromechanical properties of melilite-type piezoelectric single crystals. Journal of Applied Physics, 2015, 117, .	2.5	23

#	Article	IF	CITATIONS
73	Top-Seeded Solution Growth, Structure, Morphology, and Functional Properties of a New Polar Crystal — Cs ₂ TeW ₃ O ₁₂ . Crystal Growth and Design, 2015, 15, 4484-4489.	3.0	34
74	Flux growth, structure, and physical characterization of new disordered laser crystal LiNd(MoO4)2. Journal of Crystal Growth, 2015, 423, 1-8.	1.5	9
75	Effect of high bismuth deficiency on structure and oxide ion conductivity of a Bi _{0.55} MoO ₄ single crystal. CrystEngComm, 2015, 17, 8746-8751.	2.6	3
76	Investigations on the thermal and piezoelectric properties of fresnoite Ba2TiSi2O8 single crystals. Journal of Applied Physics, 2014, 116, .	2.5	46
77	Growth, morphology and anisotropic thermal properties of Nd-doped Sr3Y2(BO3)4 crystal. Journal of Crystal Growth, 2013, 363, 176-184.	1.5	16
78	Growth, thermal properties and laser operation of Nd:Ca_3La_2(BO_3)_4: A new disordered laser crystal. Optics Express, 2013, 21, 6091.	3.4	29
79	Composition characterization in YSGG garnet single crystals for ytterbium laser. Optical Materials Express, 2013, 3, 1408.	3.0	6
80	Polarized spectral properties and laser demonstration of Nd-doped Sr ₃ Y ₂ (BO ₃ 4 crystal. Applied Optics, 2012, 51, 7144.	1.8	21
81	Phase transfer catalyst supported, room-temperature biphasic synthesis: a facile approach to the synthesis of coordination polymers. Dalton Transactions, 2012, 41, 4320.	3.3	9
82	Growth and Piezoelectric Properties of Melilite ABC ₃ O ₇ Crystals. Crystal Growth and Design, 2012, 12, 622-628.	3.0	66
83	Growth and optical properties of Nd:LaVO4 monoclinic crystal. Journal of Materials Research, 2012, 27, 2528-2534.	2.6	8
84	Spectroscopy and laser performance of Nd:Lu_2O_3 crystal. Optics Express, 2011, 19, 17774.	3.4	35
85	Preparation, crystal structure, spectrographic characterization, thermal and third-order nonlinear optical properties of benzyltriethylammonium bis(2-thioxo-1,3-dithiole-4,5-dithiolato)aurate(III) for all-optical switching applications. Solid State Sciences, 2011, 13, 896-903.	3.2	2
86	Growth and characterization of Nd:Lu3ScxGa5â^'xO12 series laser crystals. Optics Communications, 2011, 284, 5192-5198.	2.1	11
87	Morphological study of Czochralski-grown lanthanide orthovanadate single crystals and implications on the mechanism of spiral formation. Acta Crystallographica Section A: Foundations and Advances, 2011, 67, C459-C460.	0.3	0
88	ScVO ₄ : Explorations of Novel Crystalline Inorganic Optical Materials in Rare-Earth Orthovanadate Systems. Crystal Growth and Design, 2010, 10, 4389-4400.	3.0	39
89	Morphological study of Czochralski-grown lanthanide orthovanadate single crystals and implications on the mechanism of bulk spiral formation. Journal of Applied Crystallography, 2010, 43, 308-319.	4.5	13
90	Crystal growth and thermal properties of single crystal monoclinic NdCOB (NdCa4O(BO3)3). Journal of Alloys and Compounds, 2010, 507, 335-340.	5.5	41

#	Article	IF	CITATIONS
91	Structural and thermal properties of the monoclinic Lu ₂ SiO ₅ single crystal: evaluation as a new laser matrix. Journal of Applied Crystallography, 2009, 42, 284-294.	4.5	54
92	First principles calculations of mechanical properties of the YVO4 single crystal. Journal of Applied Physics, 2007, 102, 023516.	2.5	6